Available online at www.sciencedirect.com
ScienceDirect
International Journal of Heat and Mass Transfer 51 (2008) 3190–3199
International Journal of HEAT and MASS TRANSFER
www.elsevier.com/locate/ijhmt

A general bioheat transfer model based on the theory of porous media

A. Nakayama *, F. Kuwahara

Department of Mechanical Engineering, Shizuoka University, 3-5-1 Johoku, Hamamatsu 432-8561, Japan

Received 24 October 2006; received in revised form 20 April 2007
Available online 12 September 2007

Abstract

A volume averaging theory (VAT) established in the field of fluid-saturated porous media has been successfully exploited to derive a general set of bioheat transfer equations for blood flows and its surrounding biological tissue. A closed set of macroscopic governing equations for both velocity and temperature fields in intra- and extravascular phases has been established, for the first time, using the theory of anisotropic porous media. Firstly, two individual macroscopic energy equations are derived for the blood flow and its surrounding tissue under the thermal non-equilibrium condition. The blood perfusion term is identified and modeled in consideration of the transvascular flow in the extravascular region, while the dispersion and interfacial heat transfer terms are modeled according to conventional porous media treatments. It is shown that the resulting two-energy equation model reduces to Pennes model, Wulff model and their modifications, under appropriate conditions. Subsequently, the two-energy equation model has been extended to the three-energy equation version, in order to account for the countercurrent heat transfer between closely spaced arteries and veins in the circulatory system and its effect on the peripheral heat transfer. This general form of three-energy equation model naturally reduces to the energy equations for the tissue, proposed by Chato, Keller and Seiler. Controversial issues on blood perfusion, dispersion and interfacial heat transfer coefficient are discussed in a rigorous mathematical manner.

Keywords: Bioheat transfer; Dispersion; Porous media; Volume averaging

1. Introduction

A number of bioheat transfer equations for living tissue have been proposed since the landmark paper by Pennes [1] appeared in 1948, in which the perfusion heat source was introduced. Although Pennes model is often adequate for roughly describing the effect of blood flow on the tissue temperature, some serious shortcomings exist in his model due to its inherent simplicity, as pointed out by Wulff [2], namely, assuming uniform perfusion rate without accounting for blood flow direction, neglecting the important anatomical features of the circulatory network system such as countercurrent arrangement of the system, and choosing only the venous blood stream as the fluid stream equilibrated with the tissue.

In order to overcome these shortcomings, a considerable number of modifications have been proposed by various researchers. Wulff [2] and Klinger [3] considered the local blood mass flux to account the blood flow direction, while Chen and Holmes [4] examined the effect of thermal equilibration length on the blood temperature and added the dispersion and microcirculatory perfusion terms to the Klinger equation.

All foregoing papers concerned mainly with the cases of isolated vessels and the surrounding tissue. The effect of countercurrent heat transfer between closely spaced arteries and veins in the tissue must be taken into full consideration when the anatomical configuration of the main supply artery and vein in the limbs is treated. Following the experimental study conducted by Bazett and his colleagues [5,6], Scholander and Krog [7] and Mitchell and

* Corresponding author. Tel./fax: +81 534781049.
E-mail address: tmanaka@ipc.shizuoka.ac.jp (A. Nakayama).

0017-9310/$ - see front matter © 2007 Published by Elsevier Ltd.
doi:10.1016/j.ijheatmasstransfer.2007.05.030

Nomenclature

A	surface area
A_{int}	interface between the fluid and solid
a_{f}	specific surface area
b_{ij}	Forchheimer tensor
c_p	specific heat at constant pressure
h_{f}	interfacial heat transfer coefficient
k	thermal conductivity
K_{ij}	permeability tensor
n_j	unit vector pointing outward from the fluid side to solid side
p	pressure
S_{m}	metabolic reaction rate
T	temperature
u_i	velocity vector
V	representative elementary volume
x, y	Cartesian coordinates
α	thermal diffusivity
ε	porosity
ν	kinematic viscosity
ρ	density
ω	perfusion rate
ω'	net filtration rate

Special symbols

$\tilde{\phi}$	deviation from intrinsic average
$\langle\phi\rangle$	volume average
$\langle\phi\rangle^{\text{f,s,a,v}}$	intrinsic average

Subscripts and superscripts

a	artery
dis	dispersion
f	fluid
s	solid
v	vein

Myers [8] investigated such an effect and successfully demonstrated that the countercurrent heat exchange reduces heat loss from the extremity to the surroundings, which could be quite significant due to a large surface to volume ratio. Keller and Seiler [9] established a bioheat transfer model equation to include the countercurrent heat transfer, using a one-dimensional configuration for the subcutaneous tissue region with arteries, veins and capillaries. Weinbaum and Jiji [10] proposed a new model, which is based on some anatomical understanding, considering the countercurrent arterio–venous vessels. As pointed out by Roetzel and Xuan [11], the model may be useful in describing a temperature field in a single organ, but would not be convenient to apply to the whole thermoregulation system. Excellent reviews on these bioheat transfer equations may be found in Chato [12] and Charny [13].

Khaled and Vafai [14] and Khanafer and Vafai [15] stress that the theory of porous media is most appropriate for treating heat transfer in biological tissues since it contains fewer assumptions as compared to different bioheat transfer equations. Roetzel and Xuan [11] and Xuan and Roetzel [16] exploited the volume averaging theory (VAT) previously established for the study of porous media (e.g. Cheng [17], Nakayama [18]), to formulate a two-energy equation model accounting for the thermal non-equilibrium between the blood and peripheral tissue. In their model, the perfusion term is replaced by the interfacial convective heat transfer term. This point should be examined since the interfacial convective heat transfer is different from perfusion heat transfer. Naturally, the former takes place even in the absence of the latter.

In this study, we present a rigorous mathematical development based on the volume averaging theory, so as to achieve a complete set of the volume averaged governing equations for bioheat transfer and blood flow. Most shortcomings in existing models will be overcome. We start with the case of isolated blood vessels and the surrounding tissue, to establish a two-energy equation model for the blood and tissue temperatures. We shall identify the terms describing the blood perfusion and dispersion in the resulting equation and revisit Pennes model, Wulff model and their modifications.

Subsequently, the two-energy equation model is extended to the three-energy equation model, so as to account for the effect of countercurrent heat transfer between closely spaced arteries and veins in the blood circulatory system. In this model, three individual temperatures are assigned for the arteries, veins and tissue. We shall examine the Keller and Seiler model [9] and Chato model [12] for the microcirculation as well as the model proposed by Xuan and Roetzel [16] for simulation of transient response of the human limb to an external stimulus. Controversial issues on blood perfusion, dispersion and heat transfer coefficient will be discussed in a rigorous mathematical manner.

2. Volume averaging procedure

In an anatomical view, three compartments are identified in the biological tissues, namely, blood vessels, cells and interstitium, as illustrated in Fig. 1. The interstitial space can be further divided into the extracellular matrix and the interstitial fluid. However, for sake of simplicity, we divide the biological tissue into two distinctive regions, namely, the vascular region and the extravascular region (i.e. cells and the interstitium) and treat the whole anatomical structure as a fluid-saturated porous medium, through which the blood infiltrates. The extravascular region is regarded as a solid matrix (although the extravascular fluid

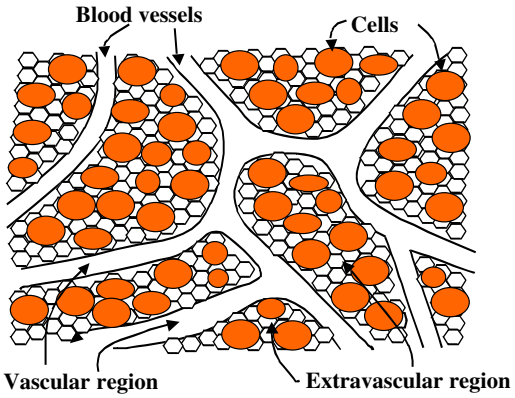

Fig. 1. Schematic view of biological tissue.

is present), and will be simply referred to the "tissue" region to differentiate it from the "blood" region.

Thus, we shall try to apply the principle of heat and fluid flow in a fluid-saturated porous medium to derive a set of the volume averaged governing equations for the bioheat transfer and blood flow. In order for the volume averaging (smoothing process) to be meaningful, we consider a control volume V in a fluid-saturated porous medium, as shown in Fig. 2, whose length scale $V^{1/3}$ is much smaller than the macroscopic characteristic length $V_c^{1/3}$, but, at the same time, much greater than the microscopic (anatomical structure) characteristic length (see e.g. Nakayama [18]). Under this condition, the volume average of a certain variable ϕ is defined as

$$\langle\phi\rangle \equiv \frac{1}{V}\int_{V_f} \phi \mathrm{d}V. \tag{1}$$

Another average, namely, intrinsic average, is given by

$$\langle\phi\rangle^f \equiv \frac{1}{V_f}\int_{V_f} \phi \mathrm{d}V, \tag{2}$$

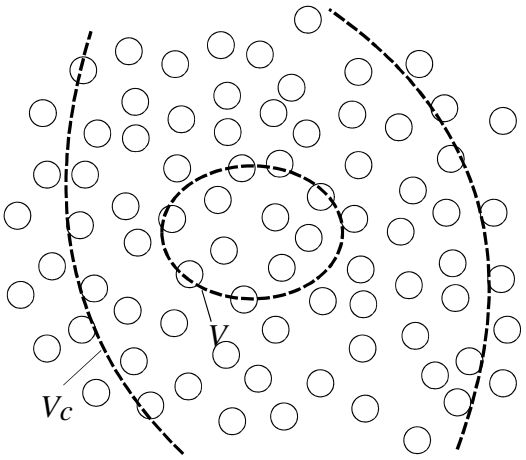

Fig. 2. Control volume in a porous medium.

where V_f is the volume space which the fluid (blood) occupies. Obviously, two averages are related as

$$\langle\phi\rangle = \varepsilon\langle\phi\rangle^f, \tag{3}$$

where $\varepsilon \equiv V_f/V$ is the local porosity, namely, the volume fraction of the vascular space, which is generally less than 0.1. Following Cheng [17], Nakayama [18], Quintard and Whitaker [19] and many others, we decompose a variable into its intrinsic average and the spatial deviation from it:

$$\phi = \langle\phi\rangle^f + \tilde{\phi}. \tag{4}$$

We shall exploit the following spatial average relationships:

$$\langle\phi_1\phi_2\rangle^f = \langle\phi_1\rangle^f\langle\phi_2\rangle^f + \langle\tilde{\phi}_1\tilde{\phi}_2\rangle^f, \tag{5}$$

$$\left\langle\frac{\partial\phi}{\partial x_i}\right\rangle = \frac{\partial\langle\phi\rangle}{\partial x_i} + \frac{1}{V}\int_{A_{int}} \phi n_i \mathrm{d}A \quad \text{or}$$

$$\left\langle\frac{\partial\phi}{\partial x_i}\right\rangle^f = \frac{1}{\varepsilon}\frac{\partial\varepsilon\langle\phi\rangle^f}{\partial x_i} + \frac{1}{V_f}\int_{A_{int}} \phi n_i \mathrm{d}A, \tag{6a, b}$$

and

$$\left\langle\frac{\partial\phi}{\partial t}\right\rangle = \frac{\partial\langle\phi\rangle}{\partial t}, \tag{7}$$

where A_{int} is the local interface between the blood and solid matrix, while n_i is the unit vector pointing outward from the fluid side to solid side. The similarity between the volume averaging and the Reynolds averaging used in the study of turbulence is quite obvious. However, it should be noted that the present volume averaging procedure is somewhat more complex than the Reynolds averaging procedure, since it involves with surface integrals, as clearly seen from (6).

We subdivide the anatomic structure into the blood phase (fluid phase) and the tissue and other solid tissue phase (solid matrix phase), in which metabolic reactions may take place. We shall consider the microscopic governing equations, namely, the continuity equation, Navier–Stokes equation and energy equation for the blood phase and the heat conduction equation for the solid matrix phase.

For the blood phase:

$$\frac{\partial u_j}{\partial x_j} = 0, \tag{8}$$

$$\frac{\partial u_i}{\partial t} + \frac{\partial}{\partial x_j}u_j u_i = -\frac{1}{\rho}\frac{\partial p}{\partial x_i} + \frac{\partial}{\partial x_j}\nu_f\left(\frac{\partial u_i}{\partial x_j} + \frac{\partial u_j}{\partial x_i}\right), \tag{9}$$

$$\rho_f c_{pf}\left(\frac{\partial T}{\partial t} + \frac{\partial}{\partial x_j}u_j T\right) = \frac{\partial}{\partial x_j}\left(k_f\frac{\partial T}{\partial x_j}\right). \tag{10}$$

For the solid matrix phase:

$$\rho_s c_s\frac{\partial T}{\partial t} = \frac{\partial}{\partial x_j}\left(k_s\frac{\partial T}{\partial x_j}\right) + S_m, \tag{11}$$

where the subscripts f and s stand for the fluid and solid, respectively. It is assumed that the fluid (blood) is incompressible and Newtonian, and all properties are constant.

3. Volume averaged continuity and momentum equations for blood flow

Let us integrate the continuity Eq. (8) over a local control volume using the formula (6b) as

$$\frac{\partial \varepsilon \langle u_j \rangle^{\mathrm{f}}}{\partial x_j} + \frac{1}{V}\int_{A_{\mathrm{int}}} u_j n_j \mathrm{d}A = 0, \tag{12}$$

where A_{int} is the local interface between the blood and solid matrix within the control volume V, while n_j is the unit vector pointing outward from the fluid side to solid side. For sake of simplicity, the porosity ε is assumed to vary moderately within a porous medium.

The second term describes the volume rate of the fluid bleeding off to the solid matrix through the interfacial vascular wall, as illustrated in Fig. 3. In most microcirculatory systems of the body, there is a net filtration of fluid from the intravascular to the extravascular compartment, such that capillary fluid filtration exceeds reabsorption. However, this would not cause fluid to accumulate within the interstitium since the lymphatic system removes excess fluid from the interstitium and returns it back to the intravascular compartment, as indicated in the figure. Thus, the second term describing the net filtration is negligibly small, such that Eq. (12) reduces to

$$\frac{\partial \langle u_j \rangle}{\partial x_j} = 0. \tag{13}$$

Accordingly, the Navier–Stokes equation (9) may be integrated to give

$$\begin{aligned}\frac{\partial \langle u_i \rangle^{\mathrm{f}}}{\partial t} + \frac{\partial}{\partial x_j}\langle u_j \rangle^{\mathrm{f}} \langle u_i \rangle^{\mathrm{f}} = &-\frac{1}{\rho_{\mathrm{f}}}\frac{\partial \langle p \rangle^{\mathrm{f}}}{\partial x_i} + \frac{\partial}{\partial x_j} v_{\mathrm{f}} \left(\frac{\partial \langle u_i \rangle}{\partial x_j} + \frac{\partial \langle u_j \rangle}{\partial x_i} \right) \\ &+ \frac{1}{V_{\mathrm{f}}}\int_{A_{\mathrm{int}}} \left(-\frac{p}{\rho} + v_{\mathrm{f}} \left(\frac{\partial u_i}{\partial x_j} + \frac{\partial u_j}{\partial x_i} \right) \right) n_j \mathrm{d}A \\ &- \frac{\partial}{\partial x_j}\langle \tilde{u}_j \tilde{u}_i \rangle^{\mathrm{f}}. \end{aligned} \tag{14}$$

In order to close the foregoing macroscopic momentum Eq. (14), the terms associated with the surface integral are modeled according to Vafai and Tien [20] as

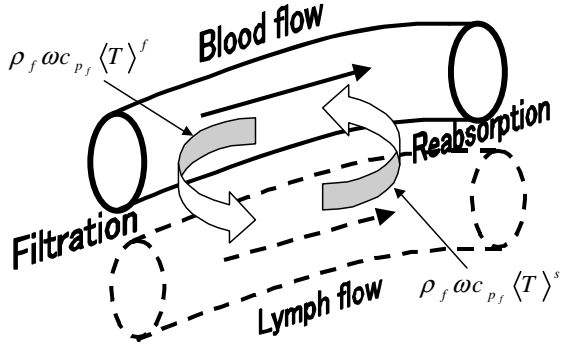

Fig. 3. Capillary blood flow and extravascular flow.

$$\begin{aligned}\frac{1}{V_{\mathrm{f}}}\int_{A_{\mathrm{int}}} \left(-\frac{p}{\rho_{\mathrm{f}}} + v_{\mathrm{f}} \left(\frac{\partial u_i}{\partial x_j} + \frac{\partial u_j}{\partial x_i} \right) \right) n_j \mathrm{d}A - \frac{\partial}{\partial x_j}\langle \tilde{u}_j \tilde{u}_i \rangle^{\mathrm{f}} \\ = -\frac{v_{\mathrm{f}}}{K}\varepsilon \langle u_i \rangle^{\mathrm{f}} - b\varepsilon^2 (\langle u_k \rangle^{\mathrm{f}} \langle u_k \rangle^{\mathrm{f}})^{1/2} \langle u_i \rangle^{\mathrm{f}} \end{aligned} \tag{15}$$

such that

$$\begin{aligned}\frac{\partial \langle u_i \rangle^{\mathrm{f}}}{\partial t} + \frac{\partial}{\partial x_j}\langle u_j \rangle^{\mathrm{f}} \langle u_i \rangle^{\mathrm{f}} = &-\frac{1}{\rho}\frac{\partial \langle p \rangle^{\mathrm{f}}}{\partial x_i} + \frac{\partial}{\partial x_j} v_{\mathrm{f}} \left(\frac{\partial \langle u_i \rangle^{\mathrm{f}}}{\partial x_j} + \frac{\partial \langle u_j \rangle^{\mathrm{f}}}{\partial x_i} \right) \\ &- \frac{v_{\mathrm{f}}}{K_{ij}}\varepsilon \langle u_j \rangle^{\mathrm{f}} - b_{ij}\varepsilon^2 \left(\langle u_k \rangle^{\mathrm{f}} \langle u_k \rangle^{\mathrm{f}} \right)^{1/2} \langle u_j \rangle^{\mathrm{f}}, \end{aligned} \tag{16}$$

where K_{ij} and b_{ij} are the permeability and Forchheimer tensors, respectively. These tensors, which depend on the anatomical structure, can be determined following the procedure established for anisotropic porous structure (Nakayama et al. [21]), as sufficient information on the anatomical structure and properties is provided For the vessels of sufficiently small diameter, the foregoing equation reduces to Darcy's law:

$$-\frac{1}{\rho}\frac{\partial \langle p \rangle^{\mathrm{f}}}{\partial x_i} - \frac{v_{\mathrm{f}}}{K_{ij}}\langle u_j \rangle = 0, \tag{17}$$

where $\langle u_j \rangle = \varepsilon \langle u_j \rangle^{\mathrm{f}}$ is the Darcian velocity (i.e. apparent velocity). We may use the Darcy law for most tissue regions except for the regions where large arteries or veins are located.

4. Two-energy equation model for blood flow and tissue

Before actually integrating the energy Eq. (10), it may be quite instructive to focus our attention on the volume average of the convection term. Using the Eqs. (5) and (6), it is straightforward to show

$$\begin{aligned}\varepsilon \left\langle \frac{\partial}{\partial x_j}\rho_{\mathrm{f}} c_{p\mathrm{f}} u_j T \right\rangle^{\mathrm{f}} = &\frac{\partial}{\partial x_j}\rho_{\mathrm{f}} c_{p\mathrm{f}} \langle u_j \rangle \langle T \rangle^{\mathrm{f}} + \frac{\partial}{\partial x_j}\varepsilon \rho_{\mathrm{f}} c_{p\mathrm{f}} \langle \tilde{u}_j \tilde{T} \rangle^{\mathrm{f}} \\ &+ \frac{1}{V}\int_{A_{\mathrm{int}}} (\rho_{\mathrm{f}} c_{p\mathrm{f}} u_j T) n_j \mathrm{d}A, \end{aligned} \tag{18}$$

where the first term on the right hand-side describes the macroscopic convection, while the second term on the right hand-side takes account of the thermal dispersion (Nakayama et al. [22]). It is the last term on the right hand-side that corresponds to the blood "perfusion" heat source. Thus, the blood perfusion heat source term is identified as an extra surface integral term resulting from changing the sequence of integration and derivation, as we obtain the macroscopic energy equation by integrating the microscopic convection term over a local control volume.

Having expanded the integrated convection term, we may readily transform both the energy Eq. (10) for the blood flow and the conduction Eq. (11) for the solid matrix into the corresponding volume averaged equations as

For the blood phase:

$$\varepsilon\rho_{\mathrm{f}}c_{p_{\mathrm{f}}}\frac{\partial\langle T\rangle^{\mathrm{f}}}{\partial t}+\rho_{\mathrm{f}}c_{p_{\mathrm{f}}}\frac{\partial}{\partial x_j}\langle u_j\rangle\langle T\rangle^{\mathrm{f}} =\frac{\partial}{\partial x_j}\left(\varepsilon k_{\mathrm{f}}\frac{\partial\langle T\rangle^{\mathrm{f}}}{\partial x_j}+\frac{k_{\mathrm{f}}}{V}\int_{A_{\mathrm{int}}}Tn_j\mathrm{d}A-\varepsilon\rho_{\mathrm{f}}c_{p_{\mathrm{f}}}\langle\tilde{u}_j\tilde{T}\rangle^{\mathrm{f}}\right) +\frac{1}{V}\int_{A_{\mathrm{int}}}k_{\mathrm{f}}\frac{\partial T}{\partial x_j}n_j\mathrm{d}A-\frac{1}{V}\int_{A_{\mathrm{int}}}\left(\rho_{\mathrm{f}}c_{p_{\mathrm{f}}}u_jT\right)n_j\mathrm{d}A. \tag{19}$$

For the solid matrix phase:

$$(1-\varepsilon)\rho_{\mathrm{s}}c_{\mathrm{s}}\frac{\partial\langle T\rangle^{\mathrm{s}}}{\partial t}=\frac{\partial}{\partial x_j}\left((1-\varepsilon)k_{\mathrm{s}}\frac{\partial\langle T\rangle^{\mathrm{s}}}{\partial x_j}-\frac{k_{\mathrm{s}}}{V}\int_{A_{\mathrm{int}}}Tn_j\mathrm{d}A\right) -\frac{1}{V}\int_{A_{\mathrm{int}}}k_{\mathrm{f}}\frac{\partial T}{\partial x_j}n_j\mathrm{d}A +\frac{1}{V}\int_{A_{\mathrm{int}}}\left(\rho_{\mathrm{f}}c_{p_{\mathrm{f}}}u_jT\right)n_j\mathrm{d}A+(1-\varepsilon)S_{\mathrm{m}}, \tag{20}$$

where $\langle T\rangle^{\mathrm{s}}$ is the intrinsic average of the solid matrix temperature. Note that the dispersion heat flux $\rho_{\mathrm{f}}c_{p_{\mathrm{f}}}\langle\tilde{u}_j\tilde{T}\rangle=\varepsilon\rho_{\mathrm{f}}c_{p_{\mathrm{f}}}\langle\tilde{u}_j\tilde{T}\rangle^{\mathrm{f}}$ appears in the volume averaged energy Eq. (19) for the blood phase, which may well be modeled under the gradient diffusion hypothesis:

$$-\varepsilon\rho_{\mathrm{f}}c_{p_{\mathrm{f}}}\langle\tilde{u}_j\tilde{T}\rangle^{\mathrm{f}}=\varepsilon k_{\mathrm{dis}_{kj}}\frac{\partial\langle T\rangle^{\mathrm{f}}}{\partial x_k} \tag{21}$$

A number of expressions have been proposed for the thermal dispersion thermal conductivity $k_{\mathrm{dis}_{kj}}$. Nakayama et al. [22] obtained a transport equation for the dispersion heat flux vector, which naturally reduces to the foregoing gradient diffusion form. For a bundle of vessels of radius R, they obtained the following expression for the predominant axial component of $k_{\mathrm{dis}_{kj}}$:

$$k_{\mathrm{dis}_{xx}}=\frac{1}{48}\left(\frac{\rho_{\mathrm{f}}c_{p_{\mathrm{f}}}\langle u\rangle^{\mathrm{f}}R}{k_{\mathrm{f}}}\right)^2k_{\mathrm{f}}\quad:\ \frac{\rho_{\mathrm{f}}c_{p_{\mathrm{f}}}\langle u\rangle^{\mathrm{f}}R}{k_{\mathrm{f}}}<1$$

(capillary blood vessels), (22a)

$$k_{\mathrm{dis}_{xx}}=2.55\left(\frac{\rho_{\mathrm{f}}c_{p}\mathrm{f}\langle u\rangle^{\mathrm{f}}R}{k_{\mathrm{f}}}\right)^{7/8}Pr^{1/8}k_{\mathrm{f}}\quad:\ \frac{\rho_{\mathrm{f}}c_{p_{\mathrm{f}}}\langle u\rangle^{\mathrm{f}}R}{k_{\mathrm{f}}}>1$$

(large arteries and veins). (22b)

In order to close the foregoing macroscopic energy Eqs. (19) and (20), the terms associated with the surface integral, describing the interfacial heat transfer and perfusion between the fluid and solid, must be modeled. For the interfacial heat transfer, Newton's cooling law may be adopted as

$$\frac{1}{V}\int_{A_{\mathrm{int}}}k_{\mathrm{f}}\frac{\partial T}{\partial x_j}n_j\mathrm{d}A=a_{\mathrm{f}}h_{\mathrm{f}}(\langle T\rangle^{\mathrm{s}}-\langle T\rangle^{\mathrm{f}}), \tag{23}$$

where a_{f} and h_{f} are the specific surface area and interfacial heat transfer coefficient, respectively. For the bundle of vascular tubes of radius R, we have $a_{\mathrm{f}}=2\varepsilon/R$ and $h_{\mathrm{f}}=Nu(k_{\mathrm{f}}/2R)$, such that $a_{\mathrm{f}}h_{\mathrm{f}}=Nu(\varepsilon k_{\mathrm{f}}/R^2)$, where Nu is the Nusselt number based on the local diameter of the vascular tube. If, the local porosity ε and specific surface area a_{f} are provided for the complex tissue–vascular structure, we may estimate the interfacial heat transfer coefficient using $h_{\mathrm{f}}=Nu(k_{\mathrm{f}}a_{\mathrm{f}}/4\varepsilon)$. Roetzel and Xuan [11] set $Nu=4.93$ for both arterial and venous blood vessels. We may appeal to a numerical experiment proposed by Nakayama et al. [23] for complex porous structures.

As for modeling the blood perfusion term, we may refer back to Fig. 3, and note that the transcapillary fluid exchange takes place between the blood and the surrounding tissue. However, the fluid lost from the vascular space will be compensated by the flow of extravascular fluids and lymph from the tissue to vascular space. It is quite reasonable to assume that extravascular fluids and all lymph in the tissue space have the same temperature as the tissue itself. Thus, we assume that the transcapillary fluid exchange takes place at the rate of ω ($\mathrm{m}^3/\mathrm{sm}^3$) and model the blood perfusion term as

$$\frac{1}{V}\int_{A_{\mathrm{int}}}\left(\rho_{\mathrm{f}}c_{p_{\mathrm{f}}}u_jT\right)n_j\mathrm{d}A=\rho_{\mathrm{f}}c_{p_{\mathrm{f}}}\omega(\langle T\rangle^{\mathrm{f}}-\langle T\rangle^{\mathrm{s}}). \tag{24}$$

Note that the perfusion rate ω, unlike that of Pennes, varies locally and we assume that its local value is provided everywhere. Pennes found that his model fits the experimental data for $\omega=2\times10^{-4}$–5×10^{-4} ($\mathrm{m}^3/\mathrm{sm}^3$).

Furthermore, the surface integral terms $\frac{k_{\mathrm{f}}}{V}\int_{A_{\mathrm{int}}}Tn_j\mathrm{d}A$ and $-\frac{k_{\mathrm{s}}}{V}\int_{A_{\mathrm{int}}}Tn_j\mathrm{d}A$ present the tortuosity heat fluxes, which are usually small, as convection dominates over conduction (see e.g. Nakayama et al. [24]). Therefore, their effects may well be absorbed in effective thermal conductivities, as done by Xuan and Roetzel [16]. Having modeled the terms associated with dispersion, interfacial heat transfer, blood perfusion and tortuosity, the individual macroscopic energy equations may finally be written for the blood and tissue phases as

For the blood phase:

$$\varepsilon\rho_{\mathrm{f}}c_{p_{\mathrm{f}}}\frac{\partial\langle T\rangle^{\mathrm{f}}}{\partial t}+\rho_{\mathrm{f}}c_{p_{\mathrm{f}}}\frac{\partial}{\partial x_j}\langle u_j\rangle\langle T\rangle^{\mathrm{f}} =\frac{\partial}{\partial x_j}\left(\varepsilon k_{\mathrm{f}}\frac{\partial\langle T\rangle^{\mathrm{f}}}{\partial x_j}+\varepsilon k_{\mathrm{dis}_{jk}}\frac{\partial\langle T\rangle^{\mathrm{f}}}{\partial x_k}\right) -a_{\mathrm{f}}h_{\mathrm{f}}(\langle T\rangle^{\mathrm{f}}-\langle T\rangle^{\mathrm{s}})-\rho_{\mathrm{f}}c_{p_{\mathrm{f}}}\omega(\langle T\rangle^{\mathrm{f}}-\langle T\rangle^{\mathrm{s}}) \tag{25}$$

in which the left hand-side term denotes the macroscopic convection term, while the four terms on the right hand-side correspond to the macroscopic conduction, thermal dispersion, interfacial convective heat transfer and blood perfusion, respectively.

For the solid tissue phase:

$$(1-\varepsilon)\rho_{\mathrm{s}}c_{\mathrm{s}}\frac{\partial\langle T\rangle^{\mathrm{s}}}{\partial t}=\frac{\partial}{\partial x_j}\left((1-\varepsilon)k_{\mathrm{s}}\frac{\partial\langle T\rangle^{\mathrm{s}}}{\partial x_j}\right)+a_{\mathrm{f}}h_{\mathrm{f}}(\langle T\rangle^{\mathrm{f}}-\langle T\rangle^{\mathrm{s}}) +\rho_{\mathrm{f}}c_{p_{\mathrm{f}}}\omega(\langle T\rangle^{\mathrm{f}}-\langle T\rangle^{\mathrm{s}})+(1-\varepsilon)S_{\mathrm{m}} \tag{26}$$

in which the left hand-side term denotes the thermal inertia term, while the four terms on the right hand-side correspond to the macroscopic conduction, interfacial convective heat transfer, blood perfusion heat source and metabolic heat source, respectively.

The resulting Eqs. (25) and (26) appear to be a correct form for the case of thermal non-equilibrium, and are expected to clear up possible confusions associated with the blood perfusion term. The continuity Eq. (13), Darcy's law (17) and the two-energy equations (25) and (26) form a closed set of the macroscopic governing equations. The present model in a multi-dimensional and anisotropic form is quite general and can be applied to find both velocity and temperature fields, as we prescribe the spatial distributions of permeability tensor, porosity, interfacial heat transfer coefficient, metabolic reaction rate and perfusion rate. It is interesting to note that, when the velocity field, porosity and metabolic reaction are prescribed, we only need to know the local value of the lumped convection–perfusion parameter, namely, $(a_f h_f + \rho_f c_{pf}\omega)$ (in addition to appropriate thermal boundary conditions) to solve the two-energy Eqs. (25) and (26) for the blood and tissue temperatures, $\langle T\rangle^f$ and $\langle T\rangle^s$.

5. Comparison of present and existing bioheat transfer models

It should be noted that most existing bioheat transfer models already reside in the present model based on the theory of porous media. We shall revisit some of the existing models and try to generate them from the present general model.

5.1. Pennes model

Pennes model [1] in our notation runs as

$$(1-\varepsilon)\rho_s c_s \frac{\partial\langle T\rangle^s}{\partial t} = \frac{\partial}{\partial x_j}\left((1-\varepsilon)k_s \frac{\partial\langle T\rangle^s}{\partial x_j}\right) + \rho_f c_{pf}\omega_{\text{Pennes}}(T_{a0} - \langle T\rangle^s) + (1-\varepsilon)S_m, \tag{27}$$

where ω_{Pennes} is the mean blood perfusion rate, while T_{a0} is the mean brachial artery temperature. We compare the Pennes model against the energy Eq. (26) for the solid tissue phase and find the following relationship:

$$\rho_f c_{pf}\omega_{\text{Pennes}}(T_{a0} - \langle T\rangle^s) = a_f h_f(\langle T\rangle^f - \langle T\rangle^s) + \rho_f c_{pf}\omega(\langle T\rangle^f - \langle T\rangle^s) \tag{28}$$

Perhaps, Pennes considered that the blood perfusion is the predominant heat source for the tissue, and did not bother to describe the interfacial convective heat transfer between the blood and tissue via the vascular wall. Instead, he introduced T_{a0} to adjust the total heat transfer, which takes place as the blood enters and leaves the tissue. We may assume $T_{a0} \simeq \langle T\rangle^f$ for small vessels, and find

$$\omega_{\text{Pennes}} \simeq \omega + \frac{a_f h_f}{\rho_f c_{pf}}. \tag{29}$$

Thus, Pennes' perfusion rate may be regarded as an effective one that includes interfacial convective heat transfer as well. Pennes assumes that blood enters the smallest vessels of the microcirculation at T_{a0}, where all heat transfer between the blood and tissue takes place. The assumption of the complete thermal equilibration with the surrounding tissue is valid only when Peclet number is sufficiently small.

5.2. Wulff model and Klinger model

Wulff [2] criticized the Pennes model, pointing out that the moving blood through a tissue convects heat in any direction, not just in the direction of the local tissue temperature gradient. He assumed that the blood temperature $\langle T\rangle^f$ is equivalent to the tissue temperature within a tissue control volume and proposed a new bioheat transfer equation. The equation later generalized by Klinger [3] runs in our notation as

$$(1-\varepsilon)\rho_s c_s \frac{\partial\langle T\rangle^s}{\partial t} = \frac{\partial}{\partial x_j}\left((1-\varepsilon)k_s \frac{\partial\langle T\rangle^s}{\partial x_j}\right) - \rho_f c_{pf}\frac{\partial\langle u_j\rangle\langle T\rangle^s}{\partial x_j} + (1-\varepsilon)S_m. \tag{30}$$

We can obtain a similar equation by combining Eqs. (25) and (26) setting $\langle T\rangle^f = \langle T\rangle^s$ as follows:

$$(\varepsilon\rho_f c_{pf} + (1-\varepsilon)\rho_s c_s)\frac{\partial\langle T\rangle^s}{\partial t} + \rho_f c_{pf}\frac{\partial}{\partial x_j}\langle u_j\rangle\langle T\rangle^s = \frac{\partial}{\partial x_j}\left((\varepsilon k_f + (1-\varepsilon)k_s)\frac{\partial\langle T\rangle^s}{\partial x_j} + \varepsilon k_{\text{dis}_{jk}}\frac{\partial\langle T\rangle^s}{\partial x_k}\right) + (1-\varepsilon)S_m. \tag{31}$$

We can easily see that the foregoing equation reduces to the Klinger equation when the ratio of vascular volume to total volume (i.e. porosity ε) is sufficiently small. Since the porosity is generally less than 0.1, the foregoing two equations are quite close to each other.

Another interpretation on the directional effect on the tissue temperature field is possible. When the blood flow is strong enough to neglect the macroscopic diffusion, the energy Eq. (25) for the blood flow reduces to

$$\rho_f c_{pf}\frac{\partial}{\partial x_j}\langle u_j\rangle\langle T\rangle^f = -a_f h_f(\langle T\rangle^f - \langle T\rangle^s) - \rho_f c_{pf}\omega(\langle T\rangle^f - \langle T\rangle^s) \tag{32}$$

Substitution of the foregoing equation into the energy equation for the tissue (26) yields the Klinger Eq. (30). The assumption implicit here is that the blood flow velocity is sufficiently high that the ratio of the bulk convection heat transfer to conduction heat transfer, namely, the Peclet number, is much greater than unity. Thus, the

Klinger model applies to the tissue with comparatively large vessels.

5.3. Cheng and Holmes model

Cheng and Holmes [4] assumed that all tissue-arterial blood heat exchange occurs along the circulatory network after the blood flows through the terminal arteries and before it reaches the level of the arterioles, which prompted them to propose the following bioheat transfer model:

$$\rho c\frac{\partial T_t}{\partial t}+\rho_{\mathrm{f}}c_{p_{\mathrm{f}}}\frac{\partial}{\partial x_j}\langle u_j\rangle T_t = \frac{\partial}{\partial x_j}\left((\varepsilon k_{\mathrm{f}}+(1-\varepsilon)k_{\mathrm{s}})\frac{\partial T_t}{\partial x_j}+k_p\frac{\partial T_t}{\partial x_j}\right) + \rho_{\mathrm{f}}c_{p_{\mathrm{f}}}\omega_j^*(T_{\mathrm{a}}^*-T_t)+(1-\varepsilon)S_{\mathrm{m}}, \tag{33}$$

where

$$\rho=\varepsilon\rho_{\mathrm{f}}+(1-\varepsilon)\rho_{\mathrm{s}}, \tag{34a}$$

$$c=(\varepsilon\rho_{\mathrm{f}}c_{p_{\mathrm{f}}}+(1-\varepsilon)\rho_{\mathrm{s}}c_{\mathrm{s}})/\rho \tag{34b}$$

and

$$T_t=(\varepsilon\rho_{\mathrm{f}}c_{p_{\mathrm{f}}}\langle T\rangle^{\mathrm{f}}+(1-\varepsilon)\rho_{\mathrm{s}}c_{\mathrm{s}}\langle T\rangle^{\mathrm{s}})/\rho c \tag{34c}$$

is the temperature of the continuum based on a volume average. Moreover, ω_j^* is the perfusion bleed-off to the tissue only from the micro-vessels past the jth generation of branching, while T_{a}^* is the blood temperature at the jth generation of branching. Both ω_j^* and T_{a}^* require the anatomical data. Chen and Holmes also take account of the "eddy" conduction due to the random flow of blood, by introducing the thermal conductivity k_p, which corresponds to our dispersion thermal conductivity k_{dis}. The energy equation similar to their Eq. (33) may be obtained by combining the two-energy equations (25) and (26) in the present model as

$$\rho c\frac{\partial T_t}{\partial t}+\rho_{\mathrm{f}}c_{p_{\mathrm{f}}}\frac{\partial}{\partial x_j}\langle u_j\rangle\langle T\rangle^{\mathrm{f}} = \frac{\partial}{\partial x_j}\left(\varepsilon k_{\mathrm{f}}\frac{\partial\langle T\rangle^{\mathrm{f}}}{\partial x_j}+(1-\varepsilon)k_{\mathrm{s}}\frac{\partial\langle T\rangle^{\mathrm{s}}}{\partial x_j}+\varepsilon k_{\mathrm{dis}_{jk}}\frac{\partial\langle T\rangle^{\mathrm{f}}}{\partial x_k}\right)+(1-\varepsilon)S_{\mathrm{m}} \tag{35}$$

When the three temperature gradients on the right hand-side are close and $\varepsilon k_{\mathrm{dis}_{jk}}=k_p\delta_{jk}$, the foregoing equation reduces to

$$\rho c\frac{\partial T_t}{\partial t}+\rho_{\mathrm{f}}c_{p_{\mathrm{f}}}\frac{\partial}{\partial x_j}\langle u_j\rangle\langle T\rangle^{\mathrm{f}} = \frac{\partial}{\partial x_j}\left((\varepsilon k_{\mathrm{f}}+(1-\varepsilon)k_{\mathrm{s}})\frac{\partial T_t}{\partial x_j}+k_p\frac{\partial T_t}{\partial x_j}\right)+(1-\varepsilon)S_{\mathrm{m}} \tag{36}$$

which is close to the equation of Chen and Holmes, except that $\rho_{\mathrm{f}}c_{p_{\mathrm{f}}}\omega_j^*(T_{\mathrm{a}}^*-T_t)$ is missing, as in the models of Wulff and Klinger, since it should vanish, as we add Eqs. (25) and (26).

6. A general three-energy equation model for countercurrent bioheat transfer

Bazett and his colleagues [6] found that the axial temperature gradient in the limb artery of human, under conditions of very low ambient temperature, is an order of magnitude higher than under normal ambient conditions. Their experimental finding brought attention to the role of countercurrent heat exchange in bioheat transfer. A schematic view of the tissue layer close to the skin surface is shown in Fig. 4, in which the arteries and veins are paired, such that the countercurrent heat transfer takes place. Mitchell and Myers [8] mathematically modeled this important role in a more general manner than that presented by Scholander and Krog [7] and demonstrated that the countercurrent heat exchange reduces heat loss from the extremity to the surroundings. However, their one-dimensional model was not able to take account of either metabolic reaction or perfusion bleed-off from the artery to vein. The foregoing survey prompts us to establish a multi-dimensional model, which can be applied to the regions of extremity, where the countercurrent heat transfer between closely spaced arteries and veins in the blood circulatory system plays an important role in the peripheral heat transfer from the extremity to the surroundings. Thus, we assign individual temperatures $\langle T\rangle^{\mathrm{a}}\langle T\rangle^{\mathrm{v}}$ and $\langle T\rangle^{\mathrm{s}}$ to the arterial blood, venous blood and tissue, respectively, to propose a general three-energy equation model as follows:

For the arterial blood phase:

$$\varepsilon_{\mathrm{a}}\rho_{\mathrm{f}}c_{p_{\mathrm{f}}}\frac{\partial\langle T\rangle^{\mathrm{a}}}{\partial t}+\rho_{\mathrm{f}}c_{p_{\mathrm{f}}}\frac{\partial}{\partial x_j}\varepsilon_{\mathrm{a}}\langle u_j\rangle^{\mathrm{a}}\langle T\rangle^{\mathrm{a}} = \frac{\partial}{\partial x_j}\left(\varepsilon_{\mathrm{a}}k_{\mathrm{a}}\frac{\partial\langle T\rangle^{\mathrm{a}}}{\partial x_j}+\varepsilon_{\mathrm{a}}k_{\mathrm{dis}a_{jk}}\frac{\partial\langle T\rangle^{\mathrm{a}}}{\partial x_k}\right)-a_{\mathrm{a}}h_{\mathrm{a}}(\langle T\rangle^{\mathrm{a}}-\langle T\rangle^{\mathrm{s}}) - \rho_{\mathrm{f}}c_{p_{\mathrm{f}}}\omega_{\mathrm{a}}'\langle T\rangle^{\mathrm{a}}. \tag{37a}$$

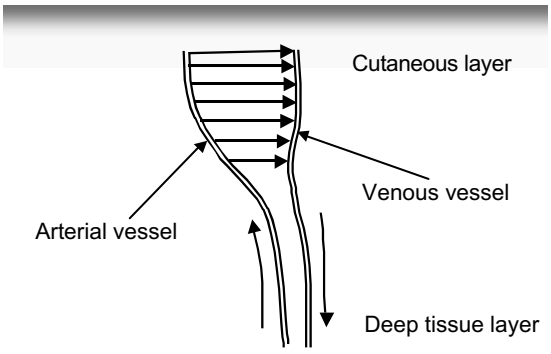

Fig. 4. Schematic view of countercurrent heat exchange near the skin surface.

For the venous blood phase:

$$\varepsilon_{\mathrm{v}}\rho_{\mathrm{f}}c_{p_{\mathrm{f}}}\frac{\partial\langle T\rangle^{\mathrm{v}}}{\partial t}+\rho_{\mathrm{f}}c_{p_{\mathrm{f}}}\frac{\partial}{\partial x_j}\varepsilon_{\mathrm{v}}\langle u_j\rangle^{\mathrm{v}}\langle T\rangle^{\mathrm{v}} = \frac{\partial}{\partial x_j}\left(\varepsilon_{\mathrm{v}}k_{\mathrm{v}}\frac{\partial\langle T\rangle^{\mathrm{v}}}{\partial x_j}+\varepsilon_{\mathrm{v}}k_{\mathrm{dis}v_{jk}}\frac{\partial\langle T\rangle^{\mathrm{v}}}{\partial x_k}\right)-a_{\mathrm{v}}h_{\mathrm{v}}(\langle T\rangle^{\mathrm{v}}-\langle T\rangle^{\mathrm{s}}) - \rho_{\mathrm{f}}c_{p_{\mathrm{f}}}\omega'_{\mathrm{v}}\langle T\rangle^{\mathrm{v}}. \tag{37b}$$

For the solid tissue phase:

$$(1-\varepsilon)\rho_{\mathrm{s}}c_{\mathrm{s}}\frac{\partial\langle T\rangle^{\mathrm{s}}}{\partial t}=\frac{\partial}{\partial x_j}\left((1-\varepsilon)k_{\mathrm{s}}\frac{\partial\langle T\rangle^{\mathrm{s}}}{\partial x_j}\right)+a_{\mathrm{a}}h_{\mathrm{a}}(\langle T\rangle^{\mathrm{a}}-\langle T\rangle^{\mathrm{s}}) + \rho_{\mathrm{f}}c_{p_{\mathrm{f}}}\omega'_{\mathrm{a}}\langle T\rangle^{\mathrm{a}}+a_{\mathrm{v}}h_{\mathrm{v}}(\langle T\rangle^{\mathrm{v}}-\langle T\rangle^{\mathrm{s}}) + \rho_{\mathrm{f}}c_{p_{\mathrm{f}}}\omega'_{\mathrm{v}}\langle T\rangle^{\mathrm{v}}+(1-\varepsilon)S_{\mathrm{m}}, \tag{38}$$

where

$$\varepsilon=\varepsilon_{\mathrm{a}}+\varepsilon_{\mathrm{v}} \tag{39}$$

Since the arterial–venous anastomoses provide direct paths from terminal arteries to veins, the net volume filtration rates of the arterial and venous vessels, ω'_{a} and ω'_{v}, are no longer negligible for the peripheral heat transfer of this kind, such that $\int_{A_{\mathrm{int}}}(\rho_{\mathrm{f}}c_{p_{\mathrm{f}}}u_jT)n_j\mathrm{d}A/V=\rho_{\mathrm{f}}c_{p_{\mathrm{f}}}\omega'\langle T\rangle^{\mathrm{f}}$. Accordingly, the velocity fields should be determined from

$$\frac{\partial\varepsilon_{\mathrm{a}}\langle u_j\rangle^{\mathrm{f}}}{\partial x_j}+\omega'_{\mathrm{a}}=0 \quad\text{and}\quad -\frac{1}{\rho}\frac{\partial\langle p\rangle^{\mathrm{a}}}{\partial x_i}-\frac{\nu}{K_{a_{ij}}}\varepsilon_{\mathrm{a}}\langle u_j\rangle^{\mathrm{a}}=0 \tag{40a, b}$$

$$\frac{\partial\varepsilon_{\mathrm{v}}\langle u_j\rangle^{\mathrm{v}}}{\partial x_j}+\omega'_{\mathrm{v}}=0 \quad\text{and}\quad -\frac{1}{\rho}\frac{\partial\langle p\rangle^{\mathrm{v}}}{\partial x_i}-\frac{\nu}{K_{\mathrm{v}_{ij}}}\varepsilon_{\mathrm{v}}\langle u_j\rangle^{\mathrm{v}}=0, \tag{41a, b}$$

where ε_{a} and ε_{v} are the volume fractions of the arterial blood and that of the venous blood, respectively. For the microcirculation of peripheral tissue in which capillaries provide a continuous connection between the terminal artery and vein (i.e. arterial–venous anastomoses), we may readily set

$$\omega'_{\mathrm{a}}=-\omega'_{\mathrm{v}} \tag{42}$$

such that the present energy equation for the solid tissue phase reduces to

$$(1-\varepsilon)\rho_{\mathrm{s}}c_{\mathrm{s}}\frac{\partial\langle T\rangle^{\mathrm{s}}}{\partial t}=\frac{\partial}{\partial x_j}\left((1-\varepsilon)k_{\mathrm{s}}\frac{\partial\langle T\rangle^{\mathrm{s}}}{\partial x_j}\right)+a_{\mathrm{a}}h_{\mathrm{a}}(\langle T\rangle^{\mathrm{a}}-\langle T\rangle^{\mathrm{s}}) + a_{\mathrm{v}}h_{\mathrm{v}}(\langle T\rangle^{\mathrm{v}}-\langle T\rangle^{\mathrm{s}}) + \rho_{\mathrm{f}}c_{p_{\mathrm{f}}}\omega'_{\mathrm{a}}(\langle T\rangle^{\mathrm{a}}-\langle T\rangle^{\mathrm{v}})+(1-\varepsilon)S_{\mathrm{m}}. \tag{43}$$

6.1. Keller and Seiler model

Keller and Seiler [9] noted that the axial temperature gradient in the limb is much higher than the transverse one and considered an energy balance within a control volume for the idealized one-dimensional steady case, as illustrated in Fig. 5, for which they proposed

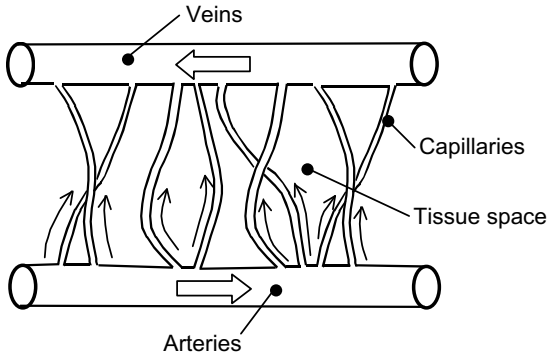

Fig. 5. One-dimensional model for countercurrent heat exchange.

$$(1-\varepsilon)k_{\mathrm{s}}\frac{\mathrm{d}^2\langle T\rangle^{\mathrm{s}}}{\mathrm{d}x^2}+a_{\mathrm{a}}h_{\mathrm{a}}(\langle T\rangle^{\mathrm{a}}-\langle T\rangle^{\mathrm{s}})+a_{\mathrm{v}}h_{\mathrm{v}}(\langle T\rangle^{\mathrm{v}}-\langle T\rangle^{\mathrm{s}}) + \rho_{\mathrm{f}}c_{p_{\mathrm{f}}}\omega'(\langle T\rangle^{\mathrm{a}}-\langle T\rangle^{\mathrm{s}})+(1-\varepsilon)S_{\mathrm{m}}=0 \tag{44}$$

which is almost identical to what we would get for the one-dimensional case from our multi-dimensional expression (43), except that the temperature difference in the perfusion term somewhat differs from ours. Keller and Seiler obtained solutions assuming that the arterial blood enters the peripheral region at the isothermal core temperature and that the venous blood is completely equilibrated with the tissue at the cutaneous layer.

6.2. Chato model

Chato's countercurrent heat transfer model [12] differs from Keller and Seiler [9] in its neglect of heat transfer between the blood and tissue. In this way, he was able to concentrate on the two temperatures instead of three as in Keller and Seiler. Chato's one-dimensional model can easily be generated from our general expressions (37a) and (37b) along with (40a) and (41a), dropping the thermal inertia and conduction terms as

$$\rho_{\mathrm{f}}c_{p_{\mathrm{f}}}\frac{\mathrm{d}}{\mathrm{d}x}\varepsilon_{\mathrm{a}}\langle u\rangle^{\mathrm{a}}\langle T\rangle^{\mathrm{a}}=-a_{\mathrm{a}}h_{\mathrm{a}}(\langle T\rangle^{\mathrm{a}}-\langle T\rangle^{\mathrm{v}})-\rho_{\mathrm{f}}c_{p_{\mathrm{f}}}\omega'_{\mathrm{a}}\langle T\rangle^{\mathrm{a}}, \tag{45a}$$

$$\rho_{\mathrm{f}}c_{p_{\mathrm{f}}}\frac{\mathrm{d}}{\mathrm{d}x}\varepsilon_{\mathrm{v}}\langle u\rangle^{\mathrm{v}}\langle T\rangle^{\mathrm{v}}=-a_{\mathrm{v}}h_{\mathrm{v}}(\langle T\rangle^{\mathrm{v}}-\langle T\rangle^{\mathrm{a}})+\rho_{\mathrm{f}}c_{p_{\mathrm{f}}}\omega'_{\mathrm{a}}\langle T\rangle^{\mathrm{a}}, \tag{45b}$$

where

$$\varepsilon_{\mathrm{a}}\langle u\rangle^{\mathrm{a}}=u_0-\omega'_{\mathrm{a}}x \quad\text{and}\quad \varepsilon_{\mathrm{a}}\langle u\rangle^{\mathrm{a}}=-u_0+\omega'_{\mathrm{a}}x. \tag{46a, b}$$

Note that u_0 is the apparent velocity at $x=0$ and that the right hand-side terms in the two Eqs. (45a) and (45b) cancels out each other, as they should for this "perfect" heat exchange system. Chato obtained arterial and venous temperature profiles along the length of the vessels and demonstrated that the effect of perfusion bleed-off is to increase the heat transfer between the vessels as compared with the case of constant mass flow rate.

6.3. Roetzel and Xuan model

Roetzel and Xuan [11] used the theory of porous media to simulate a transient response of the limb to external stimulus, in which the effect of the countercurrent heat exchange on the temperature response is expected to be significant. Their energy equation for the tissue in our notation runs as

$$(1-\varepsilon)\rho_s c_s \frac{\partial \langle T\rangle^s}{\partial t} = \frac{\partial}{\partial x_j}\left((1-\varepsilon)k_s \frac{\partial \langle T\rangle^s}{\partial x_j}\right) + a_a h_a(\langle T\rangle^a - \langle T\rangle^s) + a_v h_v(\langle T\rangle^v - \langle T\rangle^s) + (1-\varepsilon)S_m. \quad (47)$$

Comparison of the foregoing equation against our expression (43) for the tissue reveals that the perfusion term $\rho_f c_{pf}\omega'_a(\langle T\rangle^a - \langle T\rangle^v)$ is missing. Obviously, they did not retain the term describing the transcapillary fluid exchange via arterial–venous anastomoses, namely, $\int_{A_{int}} (\rho_f c_{pf} u_j T) n_j \mathrm{d}A/V = \rho_f c_{pf}\omega' \langle T\rangle^f$. If they did, they would have obtained our expression (43), which may be rearranged in their form as

$$(1-\varepsilon)\rho_s c_s \frac{\partial \langle T\rangle^s}{\partial t} = \frac{\partial}{\partial x_j}\left((1-\varepsilon)k_s \frac{\partial \langle T\rangle^s}{\partial x_j}\right) + (a_a h_a + \rho_f c_{pf}\omega'_a)(\langle T\rangle^a - \langle T\rangle^s) + (a_v h_v - \rho_f c_{pf}\omega'_a)(\langle T\rangle^v - \langle T\rangle^s) + (1-\varepsilon)S_m. \quad (48)$$

In their model, the convection–perfusion parameters, namely, $(a_f h_f \pm \rho_f c_{pf}\omega')$, are replaced by the interfacial convective heat transfer coefficients, $a_f h_f$. This difference should not be overlooked since the perfusion heat sources could be quite significant for the bioheat transfer in the extremities, as Chato [12] demonstrated using his model.

6.4. Concluding remarks

A rigorous mathematical development based on the volume averaging theory has been presented to give a correct set of bioheat transfer equations for the blood flow and its surrounding biological tissue. The blood perfusion heat source term is identified as an extra surface integral term resulting from changing the sequence of integration and derivation, as we obtain the macroscopic energy equation by integrating the microscopic convection term within a local control volume. Using this general bioheat transfer model, we have revisited existing bioheat transfer models, such as Pennes, Wulff, Klinger, Cheng and Holmes, so as to point out possible shortcomings in the models.

The two-energy equation model has been further extended to the three-energy equation model, to investigate the countercurrent heat exchange between the arterial and venous blood vessels in the circulatory system. Keller and Seiler model and Chato model may easily be generated, writing the present model for the idealized one-dimensional case. The present three-energy equation model in a multi-dimensional and anisotropic form is found to be quite general and can be applied to all regions peripheral heat transfer from the extremity to the surroundings. The three-energy equations coupled with the continuity and Darcy's laws may be solved to find both velocity and temperature fields, as we prescribe the spatial distributions of permeabilities, volume fractions, interfacial heat transfer coefficients and perfusion rates.

As pointed out by Roetzel and Xuan [11], some physiological parameters such as porosity and specific surface area depend on such factors as the body temperature and interaction with the environment, as well as vasoconstrictor and vasodilator mechanisms. These physiological parameters and model constants, which should be determined experimentally, are urgently in need. Shortage of these experimental data, however, should not hinder us from applying the present bioheat transfer model to certain cases using some estimated values. It is believed that even the applications with the estimated values do not affect explanation of the applicability of the present bioheat transfer model. Such attempts are underway.

References

[1] H.H. Pennes, Analysis of tissue and arterial blood temperature in the resting human forearm, J. Appl. Physiol. 1 (1948) 93–122.
[2] W. Wulff, The energy conservation equation for living tissue, IEEE Trans. Biomed., Eng. BME-21 (1974) 494–495.
[3] H.G. Klinger, Heat transfer in perfused biological tissue. II. The 'macroscopic' temperature distribution in tissue, Bull. Math. Biol. 40 (1978) 183–199.
[4] M.M. Chen, K.R. Holmes, Microvascular contributions in tissue heat transfer, Ann. N.Y. Acad. Sci. 335 (1980) 137–150.
[5] H.C. Bazett, L. Love, L. Eisenberg, R. Day, R.E. Forster, Temperature change in blood flowing in arteries and veins in man, J. Appl. Physiol. 1 (1948) 3–19.
[6] H.C. Bazett, E.S. Mendelson, L. Love, B. Libet, Precooling of blood in the arteries, effective heat capacity and evaporative cooling as factors modifying cooling of the extremities, J. Appl. Physiol. 1 (1948) 169–182.
[7] P.F. Scholander, J. Krog, Countercurrent heat exchange and vascular bundles in sloths, J. Appl. Physiol. 10 (1957) 405–411.
[8] J.W. Mitchell, G.E. Myers, An analytical model of the countercurrent heat exchange phenomena, Biophys. J. 8 (1968) 897–911.
[9] K.H. Keller, L. Seiler, An analysis of peripheral heat transfer in man, J. Appl. Physiol. 30 (1971) 779–789.
[10] S. Weinbaum, L.M. Jiji, A two phase theory for the influence of circulation on the heat transfer in surface tissue, in: M.K. Wells (Ed.), Advances in Boiengineering, ASME, New York, 1979, pp. 179–182.
[11] W. Roetzel, Y. Xuan, Transient response of the human limb to an external stimulus, Int. J. Heat Mass Transfer 41 (1998) 229–239.
[12] J.C. Chato, Heat transfer to blood vessels, ASME J. Biomech. Eng. 102 (1980) 110–118.
[13] C.K. Charny, Mathematical models of bioheat transfer, Advances in Heat Transfer, vol. 22, Academic Press, New York, 1992, pp. 19–155.
[14] A.-R.A. Khaled, K. Vafai, The role of porous media in modeling flow and heat transfer in biological tissues, Int. J. Heat Mass Transfer 46 (2003) 4989–5003.
[15] K. Khanafer, K. Vafai, The role of porous media in biomedical engineering as related to magnetic resonance imaging and drug delivery, Heat Mass Transfer 42 (2006) 939–953.
[16] Y. Xuan, W. Roetzel, Bioheat equation of the human thermal system, Chem. Eng. Technol. 20 (1997) 268–276.
[17] P. Cheng, Heat transfer in geothermal systems, Advances in Heat Transfer, vol. 14, Academic Press, New York, 1978, pp. 1–105.

[18] A. Nakayama, PC-aided numerical heat transfer and convective flow, CRC Press, Boca Raton, 1995.
[19] M. Quintard, S. Whitaker, One and two equation models for transient diffusion processes in two-phase systems, Adv. Heat Transfer 23 (1993) 369–465.
[20] K. Vafai, C.L. Tien, Boundary and inertia effects on flow and heat transfer in porous media, Int. J. Heat Mass Transfer 24 (1981) 195–203.
[21] A. Nakayama, F. Kuwahara, T. Umemoto, T. Hayashi, Heat and fluid flow within anisotropic porous medium, J. Heat Transfer 124 (2002) 746–753.
[22] A. Nakayama, F. Kuwahara, Y. Kodama, A thermal dispersion flux transport equation and its mathematical modelling for heat and fluid flow in a porous medium, J. Fluid Mech. 563 (2006) 81–96.
[23] A. Nakayama, F. Kuwahara, T. Hayashi, Numerical modelling for three-dimensional heat and fluid flow through a bank of cylinders in yaw, J. Fluid Mech. 498 (2004) 139–159.
[24] A. Nakayama, F. Kuwahara, M. Sugiyama, G. Xu, A two-energy equation model for conduction and convection in porous media, Int. J. Heat Mass Transfer 44 (2001) 4375–4379.